IS-PORTO 2023 PROCEEDINGS

Proceedings of the 8th International Symposium on DEFORMATION CHARACTERISTICS OF GEOMATERIALS Porto, 3rd - 6th September 2023

Numerical simulation of soil structure damage upon sampling

Lluís Monforte[1], *Marcos* Arroyo[1,2], and *Antonio* Gens[1,2]

[1]*Centre Internacional de Mètodes Numèrics en Enginyeria (CIMNE), Barcelona, Spain*
[2]*Universitat Politècnica de Catalunya (BarcelonaTECH), Barcelona, Spain*
[#]*Corresponding author: marcos.arroyo@upc.edu*

ABSTRACT

Sampling disturbance is a perennial problem of geotechnical site investigation. The structure of soft soils is particularly fragile and prone to disturbance during sampling. The extent by which different sampling procedures modify soil structure has been generally assessed on an empirical basis, observing the outcomes of tests performed on specimens obtained with different sampling technologies. That kind of experiment is slow, costly and laborious. In this communication we present a procedure to perform similar experiments "in silico", by simulating the sampling procedure, examining the effect of tube sampling on the initial soil structure, obtaining sub specimens from the simulated core and testing them afterwards in simulated triaxial undrained compression and in the oedometer. The simulations are based on G-PFEM, a code developed for soil-structure interaction at large strains. The numerical experiments clarify the origin of sampling related property variability.

Keywords: simulation, structure, damage, sampling.

1. Introduction

Disturbance of specimens recovered by tube sampling from boreholes has long been an important issue in geotechnical engineering (Hvrsolev 1949). Compared to block samples, tube sampled low to medium yield stress ratio clayey materials exhibit a decrease of strength, stiffness and preconsolidation stress, the magnitude of which depends on the sampling technique (Hvorslev 1949, Siddique et al 2000, Hight 2003, Ladd and DeGroot 2003).

The evaluation of the merits or shortcomings of each sampler geometry requires extensive field and laboratory work, a slow, costly and laborious task. Samples with different tube geometries must be extracted from the same location. Then, each sample is tested in the laboratory, in order to infer the effect of each sampling geometry on relevant design parameters, such as the peak undrained shear strength, yield stress or stiffness. This process is not exempt from uncertainty, as spatial variability of the soil in the field, transport, and preparation of the samples -among others- may influence the results.

Numerical analysis of sampling seems an attractive alternative to gather more insights into the mechanism underlying the soil disturbance caused by tube insertion. However, the numerical simulation of tube sampling is particularly difficult, not only because the large strains and contact effects experienced by the soil but also due to the very fine discretization required, that needs to be fine enough to accurately describe the geometry of the cutting shoe. As a result, and despite some efforts (Alonso et al 1981; Chopra et al 1991; Budhu and Wu 1992), the analysis of the sampling problem has practically relied only on strongly simplified models created with the Strain Path Method (Baligh, 1985; Baligh et al. 1987; Clayton et al. 1998). Recent advances on numerical simulation methods are currently opening other possibilities.

This work presents a set of numerical simulations of smooth, undrained tube insertion in structured soil using G-PFEM (Carbonell et al. 2022). The analysis illustrates the effect of the initial structure of the soil on sampling kinematics and the consequences of sampling for soil structure. These results are further employed to assess the sampler disturbance by simulating undrained triaxial and oedometer tests on material recovered from inside the tube. After discussing the relevance of the results, some conclusions are drawn.

2. Constitutive model and adopted material parameters

A broad number of constitutive models able to reproduce satisfactorily soil structure and destructuration have been proposed (Gens and Nova 1993, Liu and Carter 2002). Some of them consider anisotropy effects (Wheeler et al 2003) or even stiffness degradation with strain by employing elements of bounding surface plasticity (Rouainia and Muir Wood 2000). In the analyses reported herein, CASM-S, a modified version of CASM (Clay and Sand Model) (Yu 1998) extended to cope with structure and destructuration is used (González 2011). In CASM-S the yield surface is defined as:

$$f = \left(\frac{q}{M_\theta(p'+p_t)}\right)^2 + \frac{1}{\ln(r)}\ln\left(\frac{p'+p_t}{p_t+p_0+p_m}\right) \quad (1)$$

where p' and q are the mean effective stress and the deviatoric stress, respectively. M_θ is the slope of the

critical state line in the $p' - q$ plane, that varies with Lode's Angle (Abbo and Sloan 1995).

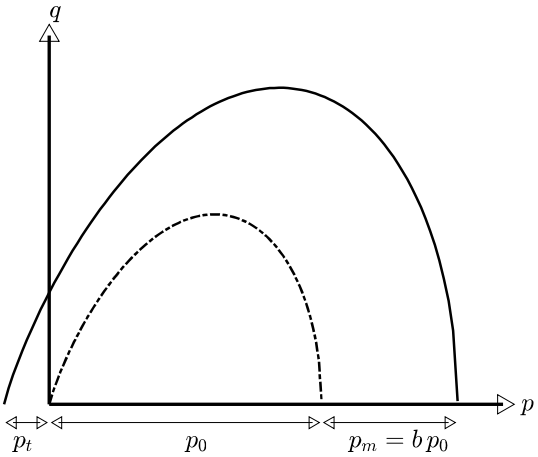

Figure 1. Graphical representation of the constitutive model

The model has three stress-like hardening variables: p_0 stands for the preconsolidation stress of the reference, unstructured soil, whereas p_t and p_m stands for the increase in the yield stress along the isotropic path in tensile and compression loading, respectively. Figure 1 shows a graphical interpretation of the yield surface.

The stress-like hardening variables representing structure are proportional to the reference preconsolidation through the bonding variable (Gens and Nova, 1993):

$$p_m = b\, p_0 \tag{2}$$

$$p_t = \alpha\, b\, p_0 \tag{3}$$

where α is a soil constitutive parameter and the bounding variable, b, evolves according to:

$$b = b_0 \exp\big(-(h - h_0)\big) \tag{4}$$

where b_0 is the initial bonding and the variable h varies with volumetric and deviatoric plastic strains as:

$$\mathrm{d}h = h_1 |\,\mathrm{tr}(\boldsymbol{l}^p)| + h_2 \sqrt{\frac{2}{3}}\, l_d^p \tag{5}$$

where $h_1$and h_2 are two constitutive parameters controlling the rate of degradation of structure in terms of volumetric and deviatoric plastic straining, $\boldsymbol{l}^p$ is the spatial plastic velocity gradient and $\mathrm{tr}(\boldsymbol{l}^p)$ and l_d^p are its volumetric and deviatoric invariants.

The reference preconsolidation stress follows the classical isotropic hardening rule of critical soil models:

$$\mathrm{d}p_0 = \frac{1+e_0}{\lambda-\kappa}\, p_0\ \mathrm{tr}(\boldsymbol{l}^p) \tag{6}$$

The model is closed with a non-associated flow rule (González 2011) and an elastic model in which the bulk and shear modulus depend linearly on the mean effective stress.

A non-local stress integration technique (Galavi and Schweiger 2010, Mánica et al 2018, Monforte et al 2019) is employed to alleviate the mesh-dependence of the solution associated with strain-localization, typical of constitutive models -such as the one employed in this work- that predict brittle behavior. To increase the robustness and computability of the model, the explicit stress integration technique (Sloan et al 2001, Monforte et al, 2014), is hosted in the general Implex technique (Oliver et al 2008; Monforte et al 2019).

Since the aim of this paper is to assess the disturbance caused by tube sampling, two different set of constitutive parameters are employed. These parameters only differ on the initial bonding, $b_0 = 1.2$ and $b_0 = 3$. The other constitutive parameters are $\lambda = 0.2$, $\kappa = 0.016$, $M = 1$, $p_0 = 250$ kPa, $n = 1.5$, $r = 2$, $h_1 = 7.5$, $h_2 = 2.3$ and $\alpha = 0.2$.

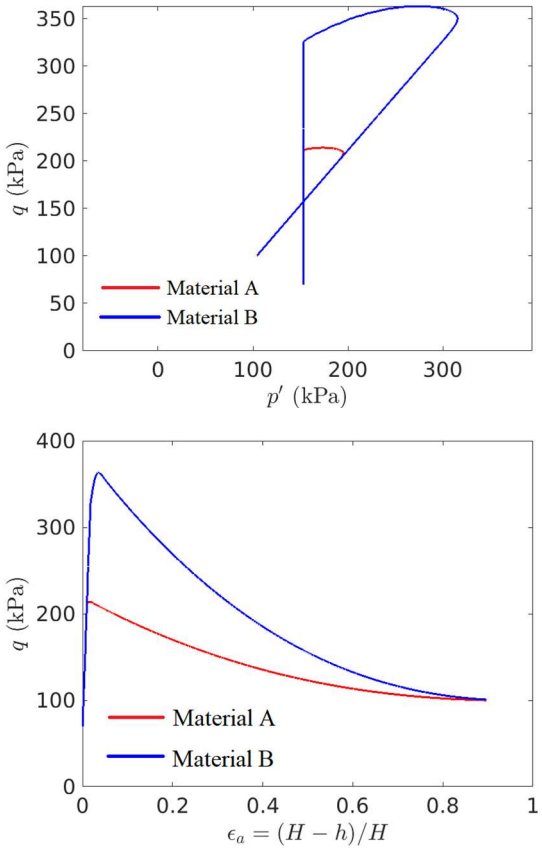

Figure 2. Simulation of undrained triaxial test: $p' - q$ plane (top) and $\epsilon_a - q$ (bottom)

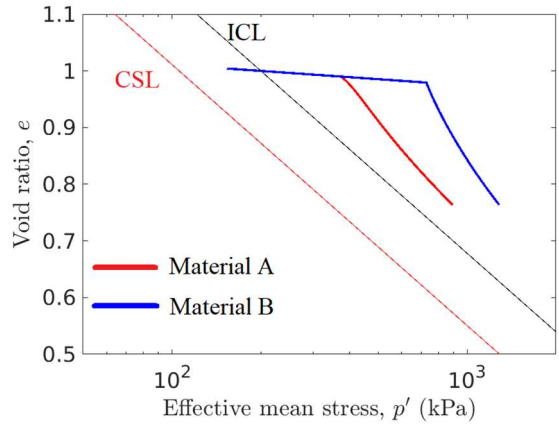

Figure 3. Simulation of oedometer test. ICL: Isotropic compression line of the reference material. CSL: Critical state line.

The effective stress path and deviatoric stress-axial deformation in undrained triaxial loading for the two sets of constitutive parameters are presented in Figure 2. In all cases, the soil has been normally consolidated to a

vertical stress of 200 kPa and a $K_0 = 0.65$, as used in the boundary value problem. These materials share the same residual undrained shear strength but have different peak undrained shear strengths.

The oedometric response is illustrated in Figure 3, that shows the evolution of the vertical stress against vertical strain. Even if p_0 is the same for both materials the initial bounding is different, and material B –with a larger initial structure– yield at higher stresses. As the material is further loaded, destructuration takes place and the void ratio tends towards the reference compression line of unstructured materials.

3. Simulation of tube sampling of structured materials

The numerical simulations of this work are carried out employing the Particle Finite Element method (PFEM) (Oñate et al 2004). PFEM is a particularly well-suited numerical tool to simulate insertion problems in geomechanics. PFEM employs a Lagrangian description of the domain, which allows to accurately model history-dependent materials, and the constant retriangulation of the finite element mesh describing the domain enables to model problems in which the domain suffers from large deformation.

Tube sampling is simulated employing an axisymmetric model using a fully coupled hydromechanical formulation. The tube is whished-in-place at a depth of 1 radius to avoid numerical problems that may arise at the first steps of the computation. The tube is pushed into the soil at 1 radius per second. Since dynamic effects are not considered and the constitutive model is not rate-dependent, this value has been selected so the soil behaves in undrained conditions. Null displacements are prescribed at the bottom of the domain, whereas null radial displacements are prescribed on the vertical boundaries of the domain. The initial effective vertical is 200 kPa and a K_0 value of 0.65 has been assumed and the soil is considered weightless. A vertical load is prescribed at the top of the domain, in equilibrium with the initial total vertical stress.

The soil is discretized with mixed, stabilized linear triangles, having displacements, Jacobian (volume change) and pore water pressure as degrees of freedom. This kind of element mitigates volumetric locking arising from both undrained conditions and incompressible constraints steaming from the effective constitutive response (Monforte et al 2017). In the nonlocal regularization technique, the characteristic length has been set to half of the thickness of the tube.

Two simulations employing the constitutive parameters previously presented are reported. The geometry of the tube is described by a diameter to wall thickness of $D/t = 20$; the tip of the tube is round. A typical discretization has around 80.000 elements and at least 20 nodes are required to have a good geometrical resolution of the cutting shoe. The computational cost of each simulation is around two days. The simulation of thinner tubes would require a larger number of elements, that would result in a higher computational cost.

To characterize the solution, Figure 4 presents the incremental plastic shear strain after a tube insertion of 2.5 diameters. The limited area of soil experiencing plastic flow extends from the cutting shoe to the axis of symmetry of the problem; the rest of the soil mass remains in the elastic regime. Moreover, the shape of the active plastic zone seems independent of the brittleness of the soil, and it is fully coincident with that obtained in the numerical simulation of non-brittle materials employing a total stress approach (Monforte et al 2022a, 2022b).

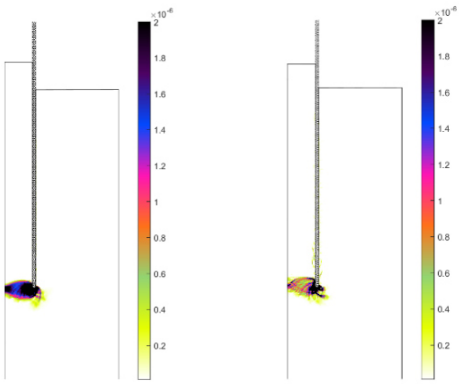

Figure 4. Contours of incremental plastic shear strain: Material A (left) and Material B (right).

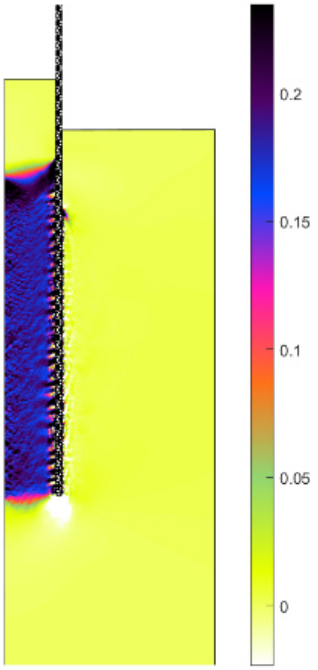

Figure 5. Contours of vertical strain: Material A.

The vertical deformation of the soil is a consequence of the plastic failure mechanism: as the tube advances, the soil that falls below the tube is diverted inside. Thus, in this region, the soil suffers from high plastic vertical extension and compression in the two horizontal directions (i.e. triaxial extension conditions), see Figure 5. Once inside of the tube, the soil remains mostly in the elastic regime, so strain changes are small. The obtained centerline strain path (not shown) is different from that predicted by the Strain path method (Baligh, 1987, Baligh et al, 1988); a discussion of the causes of this

difference can be found elsewhere (Monforte et al 2022a, 2022b).

Figure 6 characterizes the effect of sampling on the resulting structure of the soil by plotting the bonding variable, defined in Equation (4). In the adopted constitutive model, destructuration occurs due to plastic straining. As a consequence of the failure mechanism, part of the soil structure is lost as the material enters the tube. The rest of the soil mass does not suffer from substantial changes of the structure.

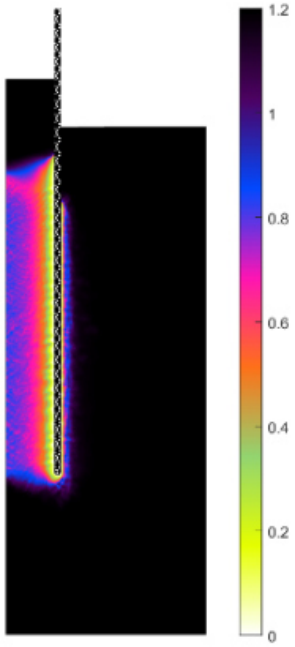

Figure 6. Contours of the bonding variable: Material A.

4. Evaluation of sampling disturbance

Sampling disturbance has been frequently inferred from the displacements and strains induced to the soil as the tube is inserted into the soil mass. For instance, Hvorslev (1949) related sampling quality to the specific recovery ratio, i.e. the incremental ratio of sample advance in the tube to sampler advance into the soil. On the other hand, since the proposal of the 'Ideal Sampling Approach' (Baligh et al, 1988) disturbance has been inferred examining the maximum vertical strain at the axis of symmetry of the problem. Monforte et al (2022a, 2022b) proposed a closed form expression relating the maximum vertical strain at the centerline of the problem in terms of the geometry of the sampler. However, it is difficult to infer disturbance of important design parameters -strength or stiffness- from the straining history.

In this work, to deduce the disturbance due to sampling, laboratory tests are simulated using the stress state (including the plastic herstory variables) of the material that has entered the tube. To this end, a region of the finite element mesh (including all variables) of the simulation of tube sampling is extracted to compute a new boundary value problem, in this case an undrained triaxial test and an oedometric loading. These boundary value problems are computed in a finite element mesh and not just in a single Gauss point as the variables, for instance bonding, are slightly heterogeneous and also because strain localization may develop during the simulation of the undrained triaxial test.

Figure 7 reports the evolution of the load versus axial deformation during unconsolidated, undrained triaxial testing. In both cases, curves for the intact soil (i.e. material in which tube sampling has not been simulated) and the sampled material are compared. The peak undrained shear strength is different between both simulations, and a reduction of around 25% can be observed in the cases in which sampling disturbance is considered. Of course, this lower peak is caused by the different available structure at the beginning of each test: the intact samples have an initial bonding variable of $b_0 = 1.2$ and $b_0 = 3.0$, whereas in the cases in which the degradation of structure caused by tube insertion is considered the bonding variable at the beginning of this value is around $b \approx 0.7$ and $b \approx 1.75$.

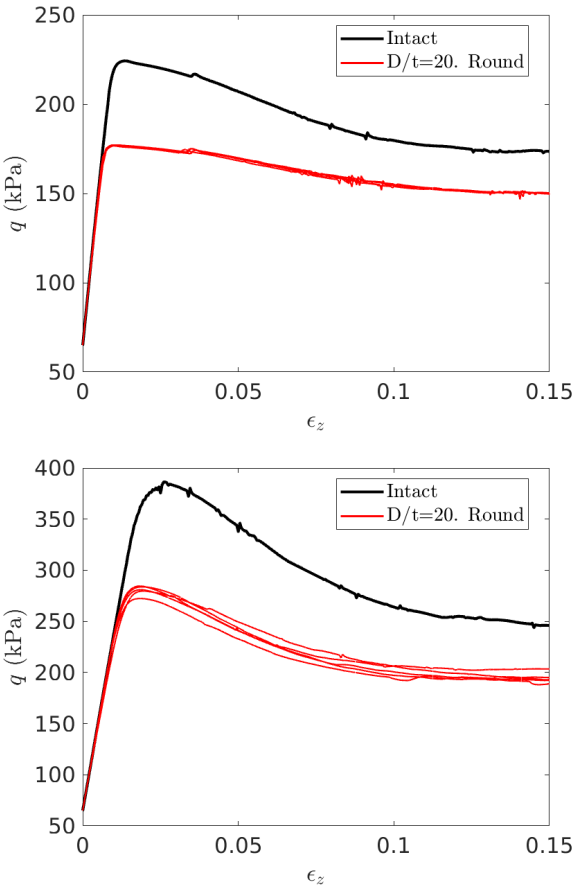

Figure 7. Stress-strain curves during undrained triaxial loading of intact and sampled material: Material A (top) and Material B (bottom).

The velocity of degradation of shear strength is similar for the intact and the sampled material, and critical state conditions cannot be identified by the end of the test.

The same exercise has been repeated, considering this time an oedometric loading. The material in which sampling disturbance has been considered yields at lower stresses levels (Figure 8). The transition between elastic and plastic behavior is abrupt for the intact material, as stresses and structure are homogeneous in the domain. This is not the case of the sampled materials, in which

spatial heterogeneities of the structure -caused by sampling- result in a slightly more gradual transition between elasticity and plasticity.

All these numerical results are consistent with current knowledge on sampling disturbance: there is a reduction of the peak undrained shear strength during triaxial loading and a reduction of the yield stress inferred during oedometric loading (Ladd and DeGroot 2003).

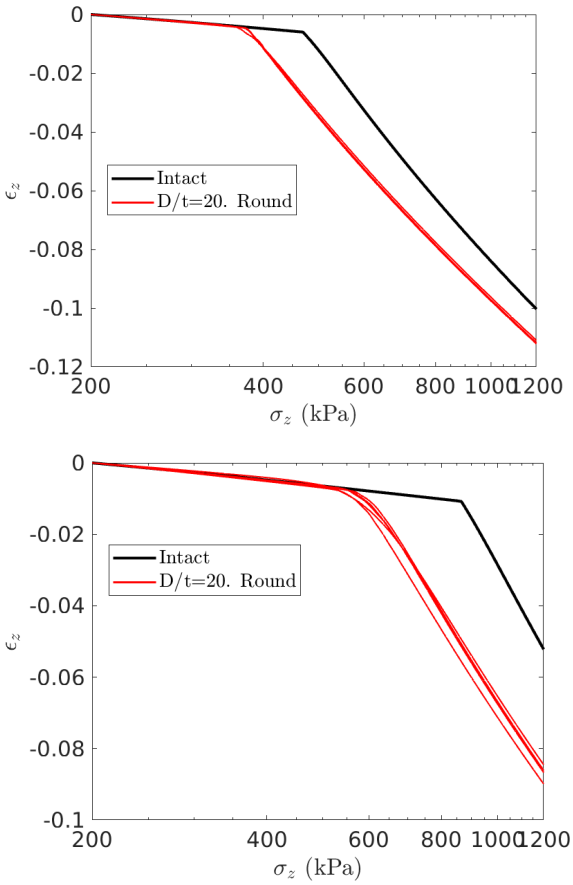

Figure 8. Oedometric response of intact and sampled material: Material A (top) and Material B (bottom).

5. Discussion

Due to the high computational demands of this type of simulation (in terms of computational cost and discretization requirements), the geometry of the tube considered in this work (thick and round-tipped) is quite different from current guidelines for practice (Hvorslev 1949, Ladd and DeGroot 2003). However, the numerical results are completely consistent with these guidelines: thick, round-tipped tubes produce drastic disturbance to the structure of soils. This degradation of structure produces a large reduction on the peak undrained shear strength and yield stress of the sampled material with respect to the intact material.

Experimental work shows that sampling may cause degradation of elastic moduli (Siddique et al 2000). This has not been observed in the numerical simulations reported in this work, as the constitutive formulation does not include that feature. To reproduce this physical phenomenon, the constitutive model needs to be extended so that changes of structure produce variations on elastic moduli (e.g. Rios et al 2015).

Even for well-maintained sampling tubes, the friction angle of the soil-steel interface is never null. In the numerical simulations reported in this work the interface has been considered fully smooth. The effects of friction on the amount of soil that enters the tube -and eventually prevents further soil from entering it- has been characterized by numerical simulations in non-brittle materials (Monforte, 2018; Monforte et al, 2023), showing that even low soil-steel rough interface behavior might cause the plugging of the tube.

Due to the rate of tube insertion (generally around 2 cm/s) it is unclear if the soil depicts an undrained behavior or partial drainage effects are relevant (especially in high permeability soils). Moreover, the constitutive response of the soil at these loading rates might show non-negligible rate effects. Both effects could be easily introduced in the simulation, which might help clarify the processes involved in sampling and the effect of the insertion rate on the disturbance of the soil.

Soil disturbance is not only caused by the insertion of the tube, but is the cumulative effect of several processes such as sampler withdrawal, transport and preparation of the sample (Ladd and DeGroot 2003). All these processes, although relevant, are not yet incorporated in the current approach.

6. Conclusions

The first attempt to assess sampling disturbance due to tube insertion using advanced numerical modelling has been reported. Tube insertion has been simulated using a constitutive model that considers structure and degradation of structure due to plastic straining. It has been shown that the material that enters the tube loses part of its structure as a consequence of the narrow localization zone that appears at the entry of the tube.

To characterize sampling disturbance, oedometer and undrained triaxial tests have been simulated using (i) material that enters the tube and (ii) intact material. A reduction of the undrained shear strength and of the yield stress has been observed, which can be ascribed to the degradation of the structure caused by sampling.

A number of basic features have been left out of the analysis, i.e. the tube has been considered completely smooth and the constitutive model does not consider changes on the elastic parameters due the degradation of structure. However, the methodology presented here offers a template for future studies on the numerical simulation of sampling disturbance.

Acknowledgements

Financial support of Ministerio de Ciencia e Innovación of Spain (MCIN/AEI/10.13039/501100011033) through the Severo Ochoa Centre of Excellence project (CEX2018-000797-S) and research project PID2020-119598RB-I00 is gratefully appreciated.

References

Abbo, A.J. and Sloan, S.W. (1995). A smooth hyperbolic approximation to the Mohr-Coulomb yield criterion.Computers & Structures 54:3, 427-441

Alonso, E. E., Oñate, E. & Casanovas, J. S. (1981). An investigation into sampling disturbance. In Proceedings of the 10th international conference on soil mechanics and foundation engineering, vol. 2, pp. 423–426. Rotterdam, the Netherlands: A. A. Balkema

Baligh, M. M. (1985). Strain path method. J. Geotech. Engng 111, No. 9, 1108–1136.

Baligh, M. M., Azzouz, A. S. & Chin, C. T. (1987). Disturbance due to 'ideal' tube sampling. J. Geotech. Engng 113, No. 7, 739–757.

Budhu, M. & Wu, C. S. (1992). Numerical analysis of sampling disturbances in clay soils. Int. J. Numer. Analyt. Methods Geomech. 16, No. 7, 467–492.

Carbonell, J. M., Monforte, L., Ciantia, M. O., Arroyo, M., & Gens, A. (2022). Geotechnical particle finite element method for modeling of soil-structure interaction under large deformation conditions. Journal of Rock Mechanics and Geotechnical Engineering, 14(3), 967-983.

Chopra, M. B., Dargush, G. F. & Banerjee, P. K. (1991). Finite deformation analysis of soil penetration problems. In Advanced geotechnical analyses: developments in soil mechanics and foundation engineering – 4 (eds P. K. Banerjee and R. Butterfield), pp. 169–222. Abingdon, UK: Taylor & Francis.

Clayton, C.R.I., Lee, J.M. and Hopper, R.J, (1998) Effects of sampler design on tube sampling disturbance – numerical and analytical investigations. Géotechnique, 48 (6), 847-867

Galavi V, Schweiger HF (2010). Nonlocal multilaminate model for strain softening analysis. Int J Geomech 2010;10(1):30–44.

Gens A, Nova R. (1993) Conceptual bases for a constitutive model for bonded soils and weak rocks. Geomechanical Engineering of Hard Soils-Soft Rocks

González, N. (2011) Development of a family of constitutive models for geotechnical applications. PhD Thesis

Hight, D. W. (2003). Sampling effects in soft clay: an update on Ladd and Lambe (1963). In Soil behavior and soft ground construction: proceedings of symposium on soil behavior and soft ground construction honoring Charles C. 'Chuck' Ladd (eds J. T. Germaine, T. C. Sheahan and R. V. Whitman), Geotechnical Special Publication 119, pp. 86–121. Reston, VA USA: American Society of Civil Engineers.

Hvorslev, M. J. (1949). Subsurface exploration and sampling of soils for civil engineering purposes. Report on a research project of the Committee on Sampling and Testing, Soil Mechanics and Foundations Division, American Society of Civil Engineers. Vicksburg, MS, USA: Waterway Experiment Station.

Ladd, C. C. & De Groot, D. J. (2003). Recommended practice for soft ground site characterization: Arthur Casagrande lecture. In Proceedings of the 12th Panamerican conference on soil mechanics and geotechnical engineering (eds P. J. Culligan, H. H. Einstein and A. J. Whittle), vol. 1, pp. 3–57. Essen, Germany: Verlag Glückauf GmbH.

Liu MD, Carter JP. (2002) A structured Cam Clay model. Can Geotech J 39(6):1313–32.

Mánica MA, Gens A, Vaunat J, Ruiz DF.(2018) Nonlocal plasticity modelling of strain localisation in stiff clays. Comput Geotech 2018;103:138–50.

Monforte, L., Carbonell, J. M., Arroyo, M. & Gens, A. (2017). Performance of mixed formulations for the particle finite element method in soil mechanics problems. Comput. Particle Mech. 4, No. 3, 269–284.

Monforte, L. (2018) Insertion Problems in Geomechanics with the Particle Finite Element Method. PhD Thesis.

Monforte, L., Ciantia, M. O., Carbonell, J. M., Arroyo, M. & Gens, A. (2019). A stable mesh-independent approach for numerical modelling of structured soils at large strains. Comput. Geotech. 116, 103215, https://doi.org/10.1016/j.compgeo.2019.103215

Monforte, L., Arroyo, M., Carbonell, J. M. & Gens, A. (2022a). Large-strain analysis of undrained smooth tube sampling. Géotechnique 116, 103215,

Monforte, L., Arroyo, M, Gens, A., Carbonell, J.M. (2022b). A new approach to evaluate the disturbance effects of soil tube sampling. Proceedings of the 20th International Conference on Soil Mechanics and Geotechnical Engineering.

Monforte, L., Arroyo, M., Carbonell, J. M. & Gens, A. (2023). Bearing capacity factors of rough, open piles. In preparation.

Oliver J, Huespe AE, Cante JC. (2008) An implicit/explicit integration scheme to increase computability of non-linear material and contact/friction problems. Comput Methods Appl Mech Eng 2008;197(21):1865–89.

Oñate E, Idelsohn SR, Del Pin F, Aubry R. (2004) The particle finite element method – an overview. Int J Comput Methods 2004;1(02):267–307.

Rios, S., Ciantia, M., Gonzalez, N., Arroyo, M., & da Fonseca, A. V. (2016). Simplifying calibration of bonded elasto-plastic models. Computers and Geotechnics, 73, 100-108.

Rouainia M, Muir Wood D (2000) D. A kinematic hardening constitutive model for natural clays with loss of structure. Géotechnique 50(2):153–64.

Siddique, A., Farooq, S. M. & Clayton, C. R. I. (2000). Disturbances due to tube sampling in coastal soils. J. Geotech. Geoenviron. Engng 126, No. 6, 568–575.

Sloan SW, Abbo AJ, Sheng D. (2001) Refined explicit integration of elastoplastic models with automatic error control. Eng Comput 18(1/2):121–94.